Available online at www.sciencedirect.com
ScienceDirect
Ceramics International 36 (2010) 1791–1795
CERAMICS INTERNATIONAL
www.elsevier.com/locate/ceramint

Transparent semiconductor zinc oxide thin films deposited on glass substrates by sol–gel process

Chien-Yie Tsay [a,*], Kai-Shiung Fan [a], Yu-Wu Wang [b], Chi-Jung Chang [c], Yung-Kuan Tseng [d], Chung-Kwei Lin [a]

[a] Department of Materials Science and Engineering, Feng Chia University, Taichung 407, Taiwan
[b] Graduate Institute of Photonics, National Changhua University of Education, Changhua 500, Taiwan
[c] Department of Chemical Engineering, Feng Chia University, Taichung 407, Taiwan
[d] Department of Cultural Heritage Conservation, National Yunlin University of Science & Technology, Yunlin 640, Taiwan

Received 21 January 2010; received in revised form 13 February 2010; accepted 2 March 2010
Available online 24 April 2010

Abstract

Transparent semiconductor ZnO thin films were spin-coated onto alkali-free glass substrates by a sol–gel process. The influence of ZnO sols synthesized via different solvents (2-ME, EtOH or IPA) on the surface morphologies, microstructures, optical properties and resistivities of the obtained films were investigated. The as-coated films were annealed in ambient air at 500 °C for 1 h. X-ray diffraction results showed all polycrystalline ZnO thin films to have preferred orientation along the (0 0 2) plane. The surface morphologies, optical transmittances and resistivity values of the sol–gel derived ZnO thin films depended on the solvent used. The ZnO thin films synthesized with IPA as the solvent exhibited the highest average transmittance 92.2%, an RMS roughness of 4.52 nm and a resistivity of $1.5 \times 10^5\ \Omega$ cm.

Keywords: A. Films; Sol–gel processes; B. Surfaces; C. Optical properties; D. ZnO

1. Introduction

Hydrogenated amorphous silicon (a-Si:H) thin films typically serve as the active channel layers in thin film transistor (TFT) arrays that drive liquid crystal displays (LCDs) and organic light-emitting device (OLED) displays. Recently, ZnO-based TFTs have been attracted much interest as potential replacements for a-Si:H TFTs. Moreover, ZnO-based TFTs also have potential applications in flexible displays [1], transparent electronics [2–4] and UV photodetecting devices [5]. ZnO is an n-type oxide semiconductor material with a direct wide bandgap (3.3 eV), large free exciton binding energy (60 mV), a wide range resistivity (10^{-4} to $10^{12}\ \Omega$ cm), high electron Hall mobility (200 $cm^2\ V\ s^{-1}$) and high transparency at room temperature [6]. Moreover, ZnO is a cheap, abundant, chemically stable and non-toxic material that has been widely used in microelectromechanical systems (MEMS), photovoltaic devices and optoelectronic devices.

Polycrystalline ZnO-based thin films have been prepared by means of various vacuum deposition techniques and chemical solution deposition processes [7]. Chemical solution deposition offers a simple, low-cost and large-area thin film coating alternative to vacuum deposition techniques. The sol–gel process is a widely known solution deposition technique. It not only provides easy, low-cost preparation of a large-area thin film, but also provides easy control over film composition and uniformity of film thickness. Moreover, oxide film thickness can be controlled by simple adjustments to solution viscosity or coating conditions.

The fabrication process for large-size TFT-LCDs continuously develops; manufacturing performance improves, the number of processing steps declines and the costs of mass production shrink. Amorphous Si TFTs have been produced by thin film deposition, photolithography and etching, but the fabrication of metal oxide TFTs by direct patterning techniques, including inkjet printing [8,9], microcontact printing [10,11] and nanoimprinting [12,13], can accomplish

* Corresponding author. Tel.: +886 4 24517250x5312; fax: +886 4 24510014.
E-mail address: cytsay@fcu.edu.tw (C.-Y. Tsay).

0272-8842/$36.00
doi:10.1016/j.ceramint.2010.03.005

the same results with a smaller number of process steps and at a lower cost. However, this economical manufacturing method needs appropriate ink materials or solution-type reagents. This work reports on the preparation of ZnO transparent semiconductor thin films by a sol–gel process and a spin-coating technique. This preparation includes solvents used to synthesize ZnO sols; these solvents have important effects on the surface morphology, crystallization, microstructure, optical properties and electrical resistivity of ZnO thin films.

2. Experimental

This research synthesized ZnO sols by taking Zn ions from a zinc acetate material that was free of chlorine ions. First zinc acetate dihydrate ($Zn(CH_3COO)_2{\cdot}2H_2O$) was dissolved in a solvent (2-methoxyethanol, ethanol or isopropyl alcohol), and then a monoethanolamine (MEA) stabilizer was added to the mixed solution. The concentration of zinc ions was 0.75 M and the molar ratio of solvent to zinc ions was maintained at 1.0. Each complex solution was stirred with a magnetic stirrer at 60 °C for 2 h to yield clear and homogenous sols. Those were aged for 48 h at room temperature before their use as coating precursors. All ZnO sol–gel films were spin-coated onto pre-cleaned glass substrates (Nippon Electric Glass OA-10 with a size of 50 mm × 50 mm) at a speed of 3000 rpm for 20 s. After which, the coated films were dried at 300 °C for 10 min, and then annealed in ambiance air at 500 °C for 1 h in a tube furnace.

The crystal structures of sol–gel derived ZnO thin films were examined by X-ray diffraction (XRD, MAC Science MXP3 X-ray diffractometer) with Cu Kα radiation. Plane views and cross-sectional views of ZnO thin film micrographs were observed via Field-Emission Scanning Electron Microscopy (FE-SEM, Hitachi S-4800). The film's surface morphologies and surface roughness levels were examined by tapping mode Scanning Probe Microscopy (SPM, Digital Instrument NS4/D3100CL/MultiMode). The optical transmittance spectra of these films were examined with a UV–vis spectrophotometer (Shimadzu UV-1601). The sheet resistances of the ZnO semiconductor thin films were measured by a contact type resistive meter (Mitsubishi Chemical Co. MCP-HT450) at room temperature.

3. Results and discussion

The crystal structures and crystallization of sol–gel derived ZnO thin films were studied by X-ray diffraction. Fig. 1 shows

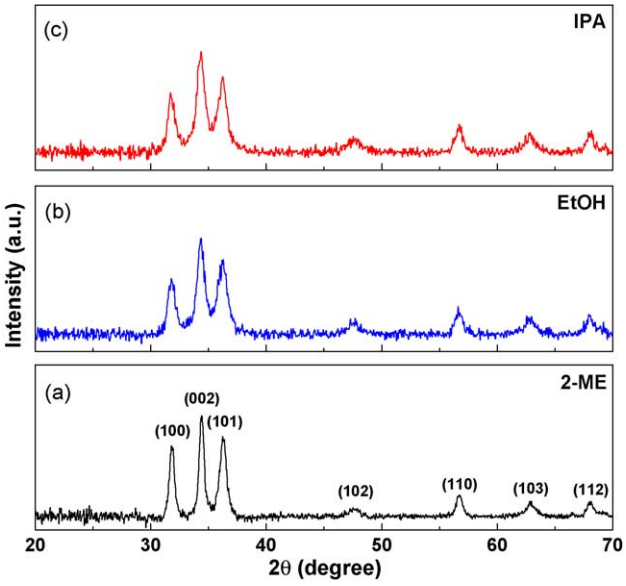

Fig. 1. X-ray diffraction patterns of sol–gel derived ZnO thin films.

the X-ray diffraction patterns of ZnO thin films synthesized by different solvents. Results show these films to be polycrystallite with a hexagonal wurzite structure and preferred orientation along the (0 0 2) basal plane. The degree of orientation of crystalline thin films collected in Table 1 have been calculated by the following formula [14]:

$$f_{(hkl)} = \frac{P(hkl) - P_0(hkl)}{1 - P_0(hkl)}, \quad (1)$$

where $f_{(h\,k\,l)}$ is the degree of $(h\,k\,l)$ orientation, $P(hkl) = I(hkl)/\sum I(hkl)$ and $P_0(hkl) = I_0(hkl)/\sum I_0(hkl)$. Here $I(h\,k\,l)$ is the $(h\,k\,l)$ peak intensity and $\sum I(hkl)$ is the sum of the intensities of all peaks in the ZnO films' diffraction data. $I_0(h\,k\,l)$ is the $(h\,k\,l)$ peak intensity and $\sum I_0(hkl)$ is the sum of the intensities of diffraction peaks in the recorded data of the standard card (JCPDS 36-1451). It can be noted that ZnO films synthesized with EtOH and IPA exhibited a higher degree of orientation of the (0 0 2) plane compared to the films synthesized with 2-ME.

Previous reports indicated that the crystal orientation of sol–gel derived ZnO active layer exerts great influence over charge transport and TFT mobility [15]. The preferential crystal orientation of sol–gel derived ZnO thin films is related to the solvents used, the MEA/Zn ratio, the sol concentration, the coating parameters (film thickness), the heat treatment

Table 1
Microstructures, optical properties and electrical resistivities of sol–gel derived ZnO thin films.

Solvents	Degree of orientation of the (0 0 2) plane	Average crystallite size (nm)	RMS roughness (nm)	Average transmittance[a] (%)	Bandgap (eV)	Resistivity (Ω cm)
2-ME	0.215	13.9	26.34	85.4	3.22	5.6×10^2
EtOH	0.232	11.5	7.06	92.1	3.26	8.6×10^4
IPA	0.234	11.6	4.52	92.2	3.27	1.5×10^5

[a] The average transmittance values were calculated the transmittance data of wavelength from 550 to 850 nm.

conditions, and the substrates used [14,16–21]. ZnO thin films possess (0 0 2) orientation because such growth is kinetically preferred. The highest density of Zn atoms is found along the (0 0 2) plane [22]; that plane possesses the higher grain-packing density [23].

The average crystallite size of the films estimated by the Scherrer's formula [24] is listed in Table 1, namely 13.9, 11.5 and 11.6 nm for films synthesized with 2-ME, EtOH and IPA, respectively. ZnO films synthesized by using the low-boiling-point solvents, EtOH and IPA, showed average crystallite sizes about 20% smaller than those films synthesized using 2-ME.

Fig. 2 shows the surface micrographs of ZnO thin films synthesized with various solvents. The plane view SEM micrograph of the ZnO film synthesized with 2-ME shows irregular fiber-like stripes and a wrinkle network (Fig. 2a). However, the micrographs of EtOH and IPA samples do not display that appearance; rather, those micrographs display superior surface flatness (Fig. 2b and c). The free surfaces of sol–gel derived ZnO thin films tend to exhibit fiber-like stripes and wrinkles when those films have undergone substantial loss of OR (hydroxy or alkoxy) groups of coating precursors [25]. Thus, a relatively smooth surface can be obtained if the starting materials provide enough OR groups.

Cross-sectional SEM micrographs of ZnO thin films (Fig. 3) show the polycrystalline ZnO films to have a granular structure and average thickness of about 170, 180 and 185 nm for films synthesized with 2-ME, EtOH and IPA, respectively. Fig. 3a and b is SEM micrographs of the 2-ME and EtOH samples; they show some nano-voids and nano-pores in the films that could degrade the quality of the film's physical properties,

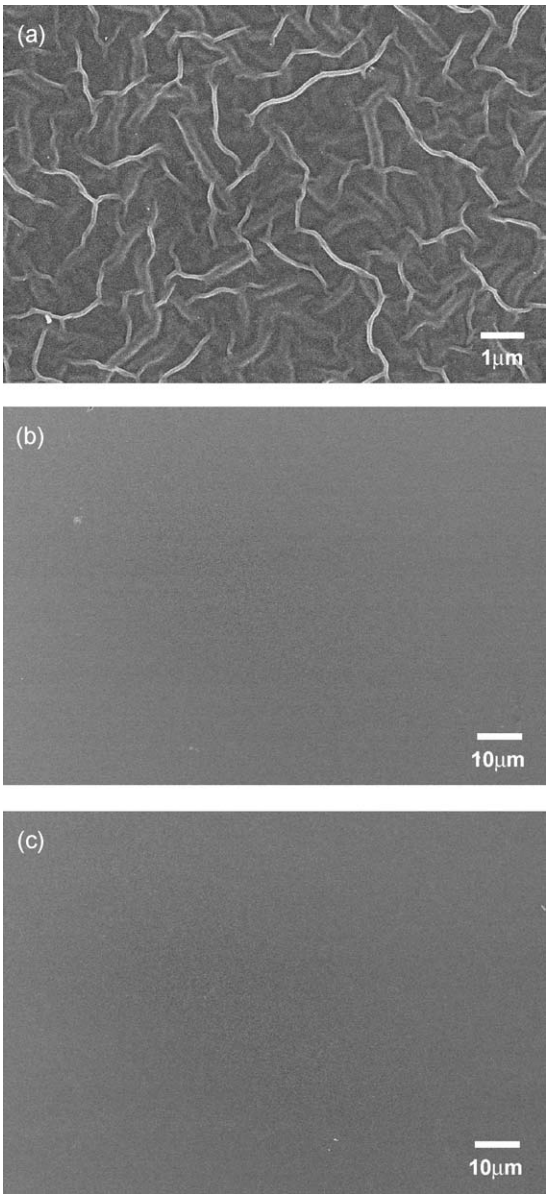

Fig. 2. Plane view SEM micrographs of ZnO thin films. These sol–gel films were synthesized from different solvents: (a) 2-ME, (b) EtOH and (c) IPA.

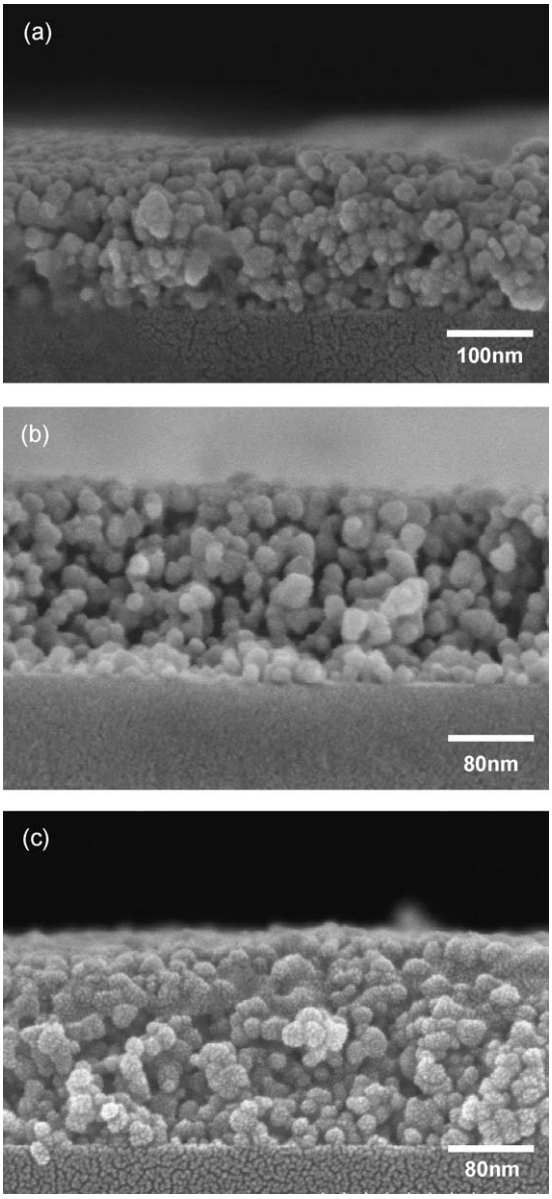

Fig. 3. Cross-sectional SEM micrographs of ZnO thin films. These sol–gel films were synthesized by means of different solvents: (a) 2-ME, (b) EtOH and (c) IPA.

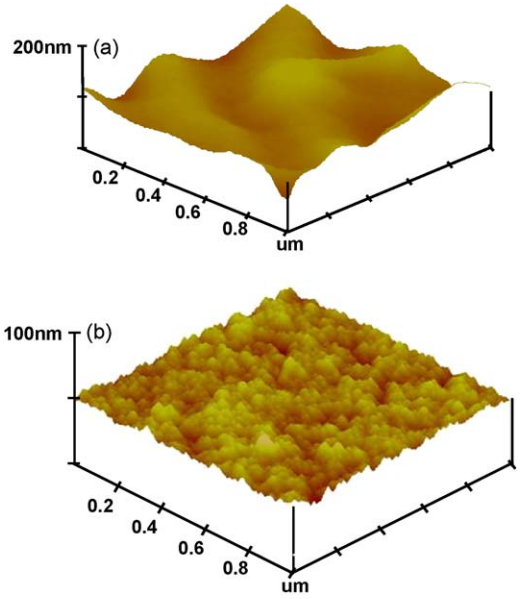

Fig. 4. SPM images of ZnO thin films that were synthesized with (a) 2-ME and (b) IPA solvents.

respectively. The ZnO thin films synthesized with IPA show superior surface flatness, more uniform film thickness, and smaller average grain size; XRD measurements confirm these results.

A SPM in tapping mode was used to examine the surface roughness of the films over a 1 μm × 1 μm area. Two SPM images of ZnO thin films (taken from 2-ME and IPA samples) shown in Fig. 4 demonstrate that the solvents used in thin film fabrication strongly influence the surface roughness of the ZnO films. The RMS roughness of these thin films is given in Table 1; thin films synthesized with EtOH and IPA had lower RMS values, because EtOH and IPA reduced the average crystallite size in the ZnO films, which produced smoother surfaces. The ZnO thin films synthesized with IPA solvent exhibited the smallest RMS value (4.52 nm) of all sol–gel derived ZnO thin films investigated in this study.

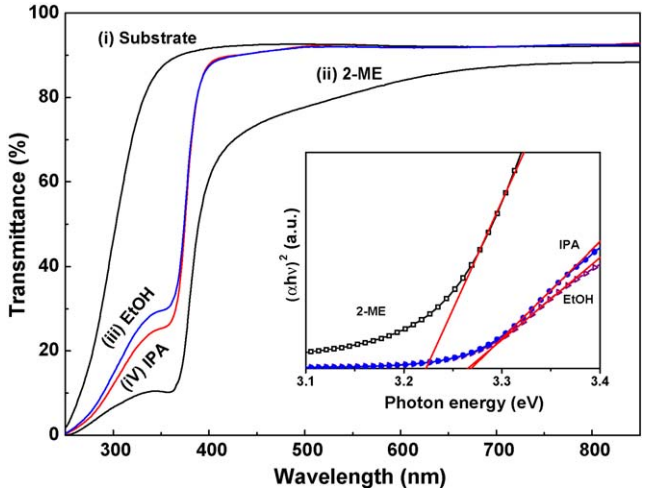

Fig. 5. Optical transmittance spectra of sol–gel derived ZnO thin films. The inset is the plot of $(\alpha h\nu)^2$ versus photon energy of thin film samples.

The optical transmittance spectra of ZnO films, with wavelengths from 250 to 850 nm (Fig. 5) exhibited sharp absorption edges in the wavelength region between 350 and 370 nm, and the EtOH and IPA samples' transmittances between 550 and 850 nm approached the transmittance of the OA-10 glass substrate, respectively. The optical transmittance spectrum of a ZnO thin film is expected to vanish in the UV region. However, in this study, optical transmittance spectra in the near UV region did not display high absorption characteristics; this may be attributed to the poor crystallinity [26] and to the nano-voids in the sol–gel derived ZnO thin films. Table 1 lists the average transmittance of the ZnO thin films; the 2-ME sample exhibited worse optical transmittance (85.4%) than the EtOH and IPA samples (>92.0%). A previous report indicated that surface flatness strongly affects the transparency of ZnO-based thin films [27]. The major reason for the poor transparency of the 2-ME sample may be that its rough surface scattered and reflected light.

The optical bandgap of a direct-transition semiconductor thin film can be obtained by the analysis of the absorption edge and application of the Tauc model [28]:

$$(\alpha h\nu) = A(h\nu - E_g)^{1/2}, \tag{2}$$

where α is the absorption coefficient, $h\nu$ is the photon energy, A is a constant and E_g is the optical bandgap. The absorption coefficient (α) in the UV region of these ZnO thin films can be calculated from $I = I_o e^{-\alpha t}$, where I is the intensity of the transmitted light, I_o is the intensity of the incident light, and t is the thickness of the thin film samples. The optical bandgaps of ZnO thin films synthesized by using various solvents were determined by extrapolation of the straight section of the plot of $(\alpha h\nu)^2$ versus photon energy (inset of Fig. 5). Table 1 lists the extrapolated bandgap values of ZnO thin films. The extrapolated E_g values of EtOH and IPA samples are close to those of previous reports (3.27 eV) [29,30], but smaller than that of ZnO crystal (3.4 eV) [6]. The bandgap difference between the thin film and crystal might be due to the grain boundaries and imperfections in the polycrystalline thin films [31].

Undoped ZnO films that possess excess interstitial ZnO ions or oxygen vacancies can contribute free electrons for electrical conduction. ZnO-TFT devices with high carrier concentration active layers exhibited high off-state currents, and have operated as n-channel depletion-mode TFTs [32]. Enhancement-mode transistors are preferable to depletion-mode transistors because it is not necessary to apply a gate voltage to switch off enhancement-mode devices. In order to produce an enhancement-mode transistor and to enhance the performance of a ZnO-TFT device, the background electron concentration must be reduced in order to increase the carrier mobility.

It was difficult to measure the Hall mobility of the ZnO semiconductor thin films potentially used as the active channel layer in the TFTs, due to their high resistivity. Therefore, their electrical properties were measured using a high resistivity meter. The resistivity of each sample can be calculated by multiplying the sheet resistances by the film thickness. Table 1

shows that the 2-ME sample exhibited a resistivity of $5.6 \times 10^2\ \Omega$ cm, and that the resistivities of the EtOH and IPA samples were 8.6×10^4 and $1.5 \times 10^5\ \Omega$ cm, respectively. The EtOH and IPA samples exhibited higher resistivities possibly due to the grain-boundary trapping of mobile carriers. ZnO film synthesized with IPA had a resistivity of 1.5×10^5; this figure was close to the values reported for films fabricated by RF magnetron sputtering [33]. For these the best field-effect mobility for ZnO-TFTs was over 2 cm V s^{-1}.

4. Conclusions

High quality, highly transparent ZnO semiconductor thin films have been successfully prepared by a sol–gel spin-coating process. All thin film samples exhibited a preferred orientation of the basal plane of wurtzite-type ZnO crystal. Compared to ZnO thin films synthesized with 2-methoxyethanol solvent, films synthesized by using solvents of ethanol or isopropyl alcohol had markedly lower surface roughness, improved transparency in the visible range, and finer average crystallite. The ZnO thin film synthesized with IPA exhibited the smallest RMS roughness, 4.52 nm, the best average transparency 92.2% and the highest resistivity, $1.5 \times 10^5\ \Omega$ cm.

Acknowledgments

The authors gratefully acknowledge that this work received financial support from the National Science Council of the Republic of China under Contract No. NSC 95-2221-E-035-006 and Taiwan TFT-LCD Association (TTLA) under Contract No. A643TT1000-S11.

References

[1] C.C. Liu, M.L. Wu, K.C. Liu, S.-H. Hsiao, Y.S. Chen, G.-R. Lin, J. Huang, Transparent ZnO thin-film transistors on glass and plastic substrates using post-sputtering oxygen passivation, J. Display Technol. 5 (2009) 192–197.
[2] S.-H.K. Park, C.-S. Hwang, M. Ryu, S. Yang, C. Byun, J. Shin, J.-I. Lee, K. Lee, M.S. Oh, S. Im, Transparent and photo-stable ZnO thin-film transistors to drive an active matrix organic-light-emitting-diode display panel, Adv. Mater. 21 (2009) 678–682.
[3] E.M.C. Fortunato, P.M.C. Barquinha, A.C.M.B.G. Pimentel, A.M.F. Gonçalves, A.J.S. Marques, L.M.N. Pereira, R.F.P. Martins, Fully transparent ZnO thin-film transistor produced at room temperature, Adv. Mater. 17 (2005) 590–594.
[4] J.F. Wager, Transparent electronics, Science 300 (2003) 1245–1246.
[5] H.S. Bae, S. Im, Ultraviolet detecting properties of ZnO-based thin film transistors, Thin Solid Films 469–470 (2004) 75–79.
[6] S.J. Pearton, D.P. Norton, K. Ip, Y.W. Heo, T. Steiner, Recent advances in processing of ZnO, J. Vac. Sci. Technol. B 22 (2004) 932–948.
[7] L. Schmidt-Mende, J.L. MacManus-Driscoll, ZnO-nanostructures, defects, and devices, Mater. Today 10 (2007) 40–48.
[8] S.T Meyers, J.T. Anderson, C.M. Hung, J. Thompson, J.F. Wager, D.A. Keszler, Aqueous inorganic inks for low-temperature fabrication of ZnO TFTs, J. Am. Chem. Soc. 130 (2008) 17603–17609.
[9] J.J. Schneider, R.C. Hoffmann, J. Engstler, O. Soffke, W. Jaegermann, A. Issanin, A. Klyszcz, A printed and flexible field-effect transistor device with nanoscale zinc oxide as active semiconductor material, Adv. Mater. 20 (2008) 3383–3387.
[10] H.-J. Lim, D.Y. Lee, Y.-J. Oh, Gas sensing properties of ZnO thin films prepared by microcontact printing, Sens. Actuators A 125 (2006) 405–410.
[11] T.L. Breen, P.M. Fryer, R.W. Nunes, M.E. Rothwell, Patterning indium tin oxide and indium zinc oxide using microcontact printing and wet etching, Langmuir 18 (2002) 194–197.
[12] C.Y. Kuan, J.M. Chou, I.C. Leu, M.H. Hon, Sol–gel-derived ZnO coating with nanopatterns fabricated by nanoimprinting, J. Am. Ceram. Soc. 91 (2008) 3160–3166.
[13] K.Y. Yang, K.-M. Yoon, K.-W. Choi, H. Lee, The direct nano-patterning of ZnO using nanoimprint lithography with ZnO–sol and thermal annealing, Microelectron. Eng. 86 (2009) 2228–2231.
[14] S. Chakrabarti, D. Ganguli, S. Chaudhuri, Substrate dependence of preferred orientation in sol–gel-derived zinc oxide films, Mater. Lett. 58 (2004) 3952–3957.
[15] B.S. Ong, C. Li, Y. Li, Y. Wu, R. Loutfy, Stable, solution-processed, high-mobility ZnO thin-film transistors, J. Am. Chem. Soc. 129 (2007) 2750–2751.
[16] M.W. Zhu, J. Gong, C. Sun, J.H. Xia, X. Jiang, Investigation of correlation between the microstructure and electrical properties of sol–gel derived ZnO based thin films, J. Appl. Phys. 104 (2008) 073113.
[17] S. O'Brien, L.H.K. Koh, G.M. Crean, ZnO thin films prepared by a single step sol–gel process, Thin Solid Films 516 (2008) 1391–1395.
[18] Y.-S. Kim, W.-P. Tai, S.-J. Shu, Effect of preheating temperature on structural and optical properties of ZnO thin films by sol–gel process, Thin Solid Films 491 (2005) 153–160.
[19] R. Ghosh, D. Basak, S. Fujihara, Effect of substrate-induced strain on the structural, electrical, and optical properties of polycrystalline ZnO thin films, J. Appl. Phys. 96 (2004) 2689–2692.
[20] L. Znaidi, G.J.A.A.S. Illia, R.L. Guennic, C. Sanchez, A. Kanaev, Elaboration of ZnO thin films with preferential orientation by a soft chemistry route, J. Sol–Gel Sci. Technol. 26 (2003) 817–821.
[21] M. Ohyama, H. Kozuka, T. Yoko, Sol–gel preparation of ZnO films with extremely preferred orientation along (0 0 2) plane from zinc acetate solution, Thin Solid Films 306 (1997) 78–85.
[22] Z. Jiwei, Z. Liangying, Y. Xi, The dielectric properties and optical propagation loss of c-axis oriented ZnO thin films deposited by sol–gel process, Ceram. Int. 26 (2000) 883–885.
[23] M. Ohyama, H. Kozuka, T. Yoko, Sol–gel preparation of transparent and conductive aluminum-doped zinc oxide films with highly preferential crystal orientation, J. Am. Ceram. Soc. 81 (1998) 1622–1632.
[24] B.D. Cullity, S.R. Stock, Elements of X-ray Diffraction, Prentice-Hall, Inc., New Jersey, 2001, p. 388.
[25] G.W. Scherer, Sintering of sol–gel films, J. Sol–Gel Sci. Technol. 8 (1997) 353–363.
[26] S.T. Tan, B.J. Chen, X.W. Sun, W.J. Fan, H.S. Kwok, X.H. Zhang, S.J. Chua, Blueshift of optical band gap in ZnO thin films grown by metal-organic chemical-vapor deposition, J. Appl. Phys. 98 (2005) 013505.
[27] J.-H. Lee, K.-H. Ko, B.-O. Park, Electrical and optical properties of ZnO transparent conducting films by the sol–gel method, J. Cryst. Growth 247 (2003) 119–125.
[28] J. Tauc, R. Grigorovici, A. Vancu, Optical properties and electronic structure of amorphous germanium, Phys. Status Solid 15 (1966) 627–637.
[29] G. Srinivasan, J. Kumar, Effect of Mn doping on the microstructures and optical properties of sol–gel derived ZnO thin films, J. Cryst. Growth 310 (2008) 1841–1846.
[30] R.E. Marotti, C.D. Bojorge, E. Broitman, H.R. Cánepa, J.A. Badán, E.A. Dalchiele, A.J. Gellman, Characterization of ZnO and ZnO:Al thin films deposited by the sol–gel dip-coating technique, Thin Solid Films 517 (2008) 1077–1080.
[31] D. Bao, H. Gu, A. Kuang, Sol–gel-derived *c*-axis oriented ZnO thin films, Thin Solid Films 312 (1998) 37–39.
[32] S. Masuda, K. Kitamura, Y. Okumura, S. Miyatake, H. Tabata, T. Kawai, Transparent thin film transistors using ZnO as an active channel layer and their electrical properties, J. Appl. Phys. 93 (2003) 1624–1630.
[33] P.F. Carcia, R.S. McLean, M.H. Reilly, G. Nunes Jr., Transparent ZnO thin-film transistor fabricated by rf magnetron sputtering, Appl. Phys. Lett. 82 (2003) 1117–1119.